

On the behavior of the Li_xNiO_2 system: an electrochemical and structural overview

C. Delmas^{a,*}, J.P. Pérès^a, A. Rougier^a, A. Demourgues^a, F. Weill^a, A. Chadwick^b,
M. Broussely^c, F. Pertion^c, Ph. Biensan^c, P. Willmann^d

^a Institut de Chimie de la Matière Condensée de Bordeaux-ICMCB-CNRS, and Ecole Nationale Supérieure de Chimie et Physique de Bordeaux, avenue Dr A. Schweitzer, 33608 Pessac Cedex, France

^b University Chemical Laboratory, University of Kent at Canterbury, Canterbury, CT2 7NH, UK

^c SAFT Advanced Battery Division, BP 1039, 86060 Poitiers, France

^d CNES, 18 avenue Edouard Belin, 31055 Toulouse Cedex, France

Accepted 16 May 1997

Abstract

Lithium nickel oxide exhibits a departure from stoichiometry ($\text{Li}_{1-z}\text{Ni}_{1+z}\text{O}_2$) consisting in the presence of extra-nickel ions within the lithium sites. Using optimized experimental synthesis conditions, compositions very close to the ideal stoichiometry ($z=0.02$) can be obtained. By using the sensitivity of the lithium site isotropic temperature factor to the stoichiometry, the amount of extra-nickel ions can be determined in a very precise way. The loss of reversibility at the first cycle is mainly related to the change in the oxidation state of the extra-nickel ions, which induces a local collapse of the structure and makes difficult the lithium re-intercalation. A systematic structural study of Li_xNiO_2 phases has been performed by extended X-ray absorption fine structure (EXAFS) as well as X-ray and electron diffraction. In the case of the starting $\text{Li}_{0.98}\text{Ni}_{1.02}\text{O}_2$ phase, a local distortion of the NiO_6 octahedra, resulting from a dynamic Jahn–Teller effect of low spin trivalent nickel ions has been evidenced from the EXAFS study. For the partially de-intercalated materials ($0.50 < x < 0.75$) which crystallize in the monoclinic system, the EXAFS study shows that the NiO_6 octahedra are only slightly distorted due to the occurrence of a hopping phenomenon between Ni^{IV} and Ni^{III} . Electron diffraction experiments show the existence of a superstructure due to a peculiar lithium-ion ordering. Systematic electrochemical studies have shown that this ordering is strongly sensitive to the presence of extra-nickel ions.
© 1997 Elsevier Science S.A.

Keywords: Lithium; Nickel oxides; Intercalation

1. Introduction

Since the discovery of the lithium–carbon battery with LiCoO_2 as the positive electrode material, a very strong interest has been devoted to lithium nickel oxide which is considerably cheaper than the homologous cobalt phase [1–7]. The preparation problems of LiNiO_2 , which have inhibited for years the development of the lithium–carbon battery with this material as the positive electrode, have been recently overcome and these batteries are now produced at the industrial scale [8]. From the fundamental point of view, numerous studies related to the material synthesis and characterization [9], to the unit cell modifications induced by the lithium de-intercalation [10,11], and to the effect of various substituting cations have been reported [12–17]. Several structural tran-

sitions occur within the reversible intercalation/de-intercalation domain ($0.30 < x < 1.0$). A monoclinic solid solution is observed in a wide composition domain ($0.50 < x < 0.75$). As suggested by the following remarks, the properties of this monoclinic phase seem to play a key role in the electrochemical behavior of the Li_xNiO_2 electrode: (i) the cell polarization is smaller for this material than for border phases with rhombohedral symmetry, and (ii) on long range cycling (1200 cycles) the most part of the capacity is actually obtained by cycling inside the monoclinic domain [7]. In our laboratories, we have tried to understand, in a very precise way, the relation between the electrochemical behavior, the composition of the pristine material, the oxidation process and the structural modifications both at the short and long range scale. The purpose of this paper is to give an overview of new results which relate to the relationship between composition, structure and electrochemical behavior. A special

* Corresponding author.

interest is focused on the structural comparison between $\text{Li}_{0.98}\text{Ni}_{1.02}\text{O}_2$ pristine phase and $\text{Li}_{0.63}\text{Ni}_{1+z}\text{O}_2$ obtained by electrochemical de-intercalation of lithium.

2. Results and discussion

2.1. X-ray diffraction study of $\text{Li}_{1-z}\text{Ni}_{1+z}\text{O}_2$ phases

As the electrochemical behavior is strongly related to the departure from stoichiometry, a systematic X-ray characterization method has been developed from the Rietveld refinement technique (Fullprof program) in order to determine the amount of extra-nickel ions for many materials in a very reproducible way [9]. A systematic study has thus been carried out on $\text{LiNi}_{1-y}\text{Co}_y\text{O}_2$ and $\text{Li}_{1-z}\text{Ni}_{1+z}\text{O}_2$ phases. In the case of the cobalt system, there is no irreversibility at the first cycle if the cobalt amount is larger than or equal to 0.30; therefore, one can assume that the structure is strictly bidimensional. Rietveld refinement of the X-ray diffraction (XRD) pattern of the $\text{LiNi}_{0.70}\text{Co}_{0.30}\text{O}_2$ phase, with an ideal two-dimensional (2D) structure, gives very decent values of the isotropic thermal agitation parameter at the lithium site ($B(\text{Li}) = 1.2(3) \text{ \AA}^2$ [18]). For materials with a departure from the ideal stoichiometry, the $B(\text{Li})$ values are negative and the absolute value of $B(\text{Li})$ can be related to the amount of extra-nickel ions in the lithium sites. This negative value reflects the presence within the lithium sites of an electronic density larger in the material than in the actual 2D-structural hypothesis. Therefore, Rietveld refinements, where the isotropic thermal agitation parameter at the lithium site $B(\text{Li})$ is fixed (equal to 1.2) and the amount of extra-nickel ions (z) is free, can be achieved in a very reproducible way. All $\text{Li}_{1-z}\text{Ni}_{1+z}\text{O}_2$ phases obtained in various experimental conditions were systematically characterized; the smallest departure from stoichiometry ($0.015 < z < 0.020$) has been observed for materials obtained at 700°C with Li_2O or LiOH as the lithiating agent [9,7].

One must note that, while the XRD is very sensitive to the presence of a small amount of nickel ions within the lithium site, it is impossible to get significant results about the possible absence of some nickel ions in the NiO_2 slab resulting from a lithium/nickel exchange. Recently, neutron diffraction experiments have shown that this exchange does not occur in classical synthesis conditions [19].

Another interesting point which can be discussed from the structural data concerns the variation of the slab and interslab thickness versus the extra-nickel ion amount. The departure from the ideal stoichiometry results from the presence of $2z$ divalent nickel ions within the material; half of them are in the NiO_2 slab, while the other half are in the interslab space. When the extra-nickel ion amount increases, the larger size of the Ni^{II} ions versus the Ni^{III} one increases the slab thickness and, simultaneously, the interslab thickness decreases as the result of the presence of the smaller Ni^{II} (versus Li^+) within the lithium site. Therefore, the structural study of the starting material shows unambiguously that the presence of extra-

nickel ions within the lithium site renders lithium diffusion more difficult.

2.2. Electrochemical behavior and loss of reversibility at the first cycle

The Li_xNiO_2 electrode exhibits a very good reversibility except for the first cycle where a significant part of the charged capacity is not recovered at the first discharge. The extent of this irreversibility, which must match with that of the negative carbon electrode, is related to the departure from stoichiometry of the starting $\text{Li}_{1-z}\text{Ni}_{1+z}\text{O}_2$ phase. Nevertheless, the relationship between the number of extra-nickel ions and the number of lithium ions which cannot be re-intercalated at the first discharge is difficult to describe. Compilation of data related to the electrochemical behavior of $\text{Li}_{1-z}\text{Ni}_{1+z}\text{O}_2$ and $\text{LiNi}_{1-y}\text{Co}_y\text{O}_2$ phases shows that even a small amount of extra-nickel ions plays a dramatic role on the cell capacity: for example the $\text{Li}_{0.95}\text{Ni}_{1.05}\text{O}_2$ material has a poor exchanged capacity which forbids any practical use. In order to try to understand what goes on, a systematic electrochemical study has been performed for various z values and in each case for increasing de-intercalation amounts [20]. Fig. 1 gives some of these results as example; from these global data the following remarks can be drawn: (i) if

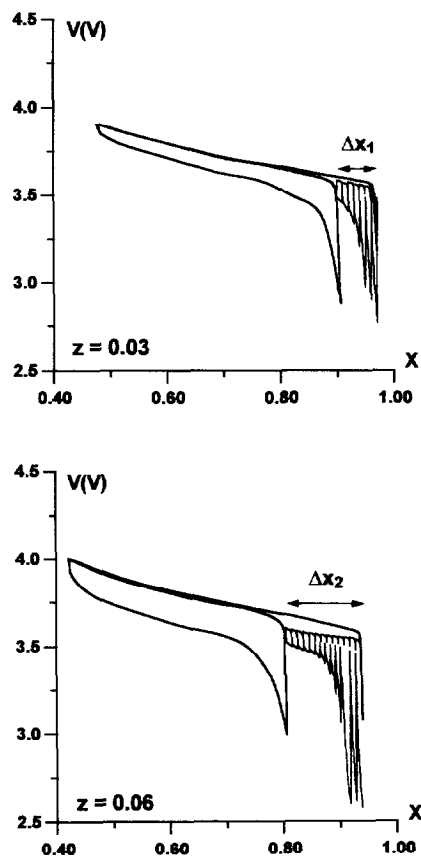


Fig. 1. Correlation between the reversible composition range and the loss of reversibility at the first cycle. Effect of the extra-nickel ions amount. In each case two cycling curves have been superimposed. The cycle around the starting composition is made in open-circuit voltage conditions in order to decrease the kinetics effects.

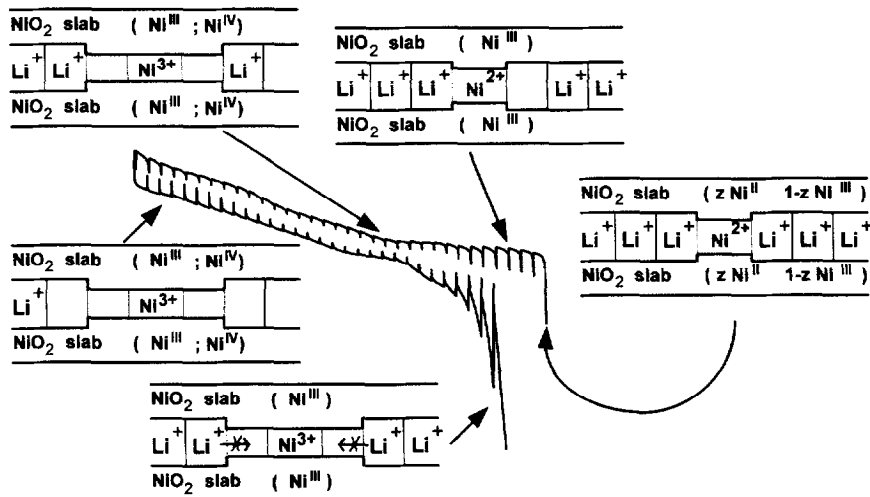


Fig. 2. Changes in oxidation state of nickel ions during the first electrochemical cycle. The oxidation of Ni^{II} induces a local collapse of the interslab space which makes difficult the lithium re-intercalation.

only few lithium ions are de-intercalated the reversibility is very good; (ii) the de-intercalation range related to this reversibility increases with z ; (iii) if this limit is exceeded the classical loss of reversibility is observed, and (iv) the initial capacity can be partially recovered if a deep discharge to low potential and at low rate is performed up to the starting $\text{Li}_{1-z}\text{Ni}_{1+z}\text{O}_2$ composition. All these data show that the loss of reversibility is related to the intercalation/de-intercalation kinetics and not to thermodynamical limitations. The overall behavior can be explained using the model schematized in Fig. 2. At the beginning of the first de-intercalation, only the divalent nickel ions of the slabs are oxidized to the trivalent state; therefore, there is no limitation to the re-intercalation process at the next discharge. On the contrary, if a larger amount of lithium is de-intercalated, the extra-nickel ions are oxidized to the trivalent state leading to a local collapse of the interslab space. As a result, the 6 lithium sites around such each extra-nickel ion can hardly be re-intercalated. In classical cycling conditions, the cell polarization when these sites are concerned prevents the lithium re-intercalation for a given cut-off voltage. Nevertheless, at very low rate these sites can be re-intercalated. Even though such a cycling allows to recover the starting material, the overall cycleability of the cell is strongly affected. One can assume that, because of the existence of intercalation gradients, the $\text{Li}_{1-z}\text{Ni}_{1+z}\text{O}_2$ composition must be exceeded on the grain surface; therefore, if a small amount of the over-intercalated phase ($\text{Li}_{1+\Delta}\text{NiO}_2$) is formed on the particle surface, the poor electrochemical reversibility of this material leads to a strong increase of the cell polarization on further cycling.

2.3. XRD study of the structure of the de-intercalated $\text{Li}_{0.63}\text{Ni}_{1.02}\text{O}_2$ phase

$\text{Li}_{0.63}\text{Ni}_{1.02}\text{O}_2$ obtained by electrochemical de-intercalation of the $\text{Li}_{0.98}\text{Ni}_{1.02}\text{O}_2$ phase has been studied by XRD. This material crystallizes in the monoclinic system ($C2/m$ space

group) with the following unit cell parameters: $a_{\text{mon.}} = 4.9883(6) \text{ \AA}$, $b_{\text{mon.}} = 2.8282(4) \text{ \AA}$, $c_{\text{mon.}} = 5.0691(8) \text{ \AA}$, $\beta = 109.75(1)^\circ$ [21]. The Rietveld refinement, realized in the same experimental conditions as for the starting phase, also leads to 2% extra-nickel ions in the lithium site. This result shows clearly that the integrity of the NiO_2 slab is preserved upon de-intercalation contrary to what is observed in the case of the Li_xMnO_2 system [22]. The Ni–O distances deduced from the refined atomic positions show only a very weak octahedron distortion (4 short bonds ($1.920(3) \text{ \AA}$) and 2 long ones ($1.953(3) \text{ \AA}$)). This structural distortion, which is of a very small amplitude in comparison to that of NaNiO_2 (1.952 and 2.168 \AA ; [23]), suggests that the Jahn–Teller effect is certainly not the origin of the macroscopic lattice distortion. Since the XRD gives only the average long range structure, an EXAFS study has been carried out to characterize precisely the Ni–O bond length distribution.

2.4. EXAFS study of the local structure of $\text{Li}_{0.98}\text{Ni}_{1.02}\text{O}_2$ and $\text{Li}_{0.63}\text{Ni}_{1.02}\text{O}_2$

Contrary to NaNiO_2 , which exhibits a monoclinic distortion due to the Jahn–Teller effect of low spin trivalent nickel ions, LiNiO_2 crystallizes in the rhombohedral system even at low temperature, while $\text{Li}_{0.63}\text{Ni}_{1.02}\text{O}_2$ exhibits a monoclinic distortion. For this material, it is difficult to conceive that the Jahn–Teller effect is strong enough to distort the structure at the macroscopic scale since the hopping between Ni^{IV} and Ni^{III} ions is expected to inhibit the occurrence of a macroscopic distortion. In order to detect the possible existence of a local distortion of the NiO_6 octahedra, EXAFS experiments have been performed on both $\text{Li}_{0.98}\text{Ni}_{1.02}\text{O}_2$ [24] and $\text{Li}_{0.63}\text{Ni}_{1.02}\text{O}_2$ phases both at room and at liquid nitrogen temperatures [21].

Fig. 3 gives a comparison of the Fourier-transform of the Ni K-edge EXAFS signals ($k_{\text{min.}} = 4 \text{ \AA}^{-1}$; $k_{\text{max.}} = 15 \text{ \AA}^{-1}$) obtained for both $\text{Li}_{0.98}\text{Ni}_{1.02}\text{O}_2$ and $\text{Li}_{0.63}\text{Ni}_{1.02}\text{O}_2$ phases at

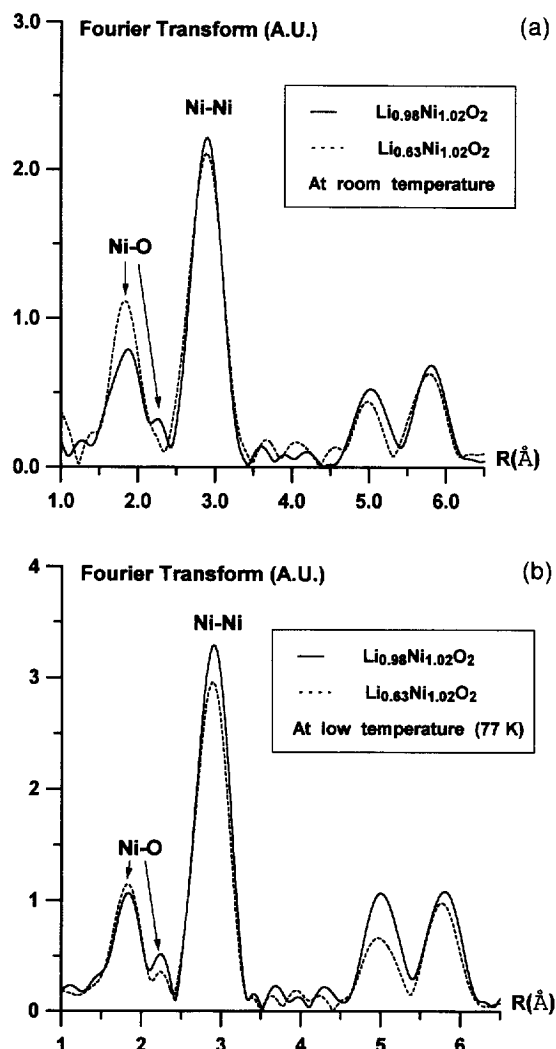


Fig. 3. Experimental Fourier-transforms for Ni K-edge EXAFS signals of $\text{Li}_{0.98}\text{Ni}_{1.02}\text{O}_2$ and $\text{Li}_{0.63}\text{Ni}_{1.02}\text{O}_2$: (a) at room temperature, and (b) at liquid nitrogen temperature.

room and at liquid nitrogen temperatures. Two main shells are observed: the first one relative to the Ni–O distances is split in the case of $\text{Li}_{0.98}\text{Ni}_{1.02}\text{O}_2$ whatever the temperature, while in the case of the $\text{Li}_{0.63}\text{Ni}_{1.02}\text{O}_2$ phase a visible splitting is only observed at low temperature. The second shell relative to the Ni–Ni distances is never split. In all cases, these shells have been refined. For the $\text{Li}_{0.98}\text{Ni}_{1.02}\text{O}_2$ phase, at both temperatures, the fit leads to 4 short distances at 1.91 Å and two long distances at 2.07 Å corresponding to an average Ni–O distance of 1.96 Å in good agreement with XRD analysis. These values clearly indicate the occurrence of an NiO_6 octahedron distortion related to a Jahn–Teller effect. In the case of the de-intercalated phase, comparison of the fit results, by considering the two kinds of distribution (one shell (6 Ni–O distances) or two shells (4 + 2 Ni–O distances)), clearly indicates that some of the NiO_6 octahedra are distorted like in the case of the pristine phase. Moreover, the number of distorted NiO_6 octahedra slightly increases when the temperature decreases. The refinement results show that at low temperature the ‘ $\text{Ni}^{\text{III}}\text{O}_6$ ’ octahedra are distorted. When the

temperature increases, only a part of them remains distorted as a result of the $\text{Ni}^{\text{IV}}\text{–O–Ni}^{\text{III}}$ hopping which tends to inhibit the Jahn–Teller effect.

In all cases, the fit of the shell relative to the Ni–Ni distances gives only one distance even in the case of the $\text{Li}_{0.63}\text{Ni}_{1.02}\text{O}_2$ phase where two slightly different distances are deduced from the crystallography results (2.83 and 2.86 Å). These distances are certainly too close to each other to be resolved by EXAFS experiments. This result shows that the NiO_6 octahedron distortion remains at the local scale.

In conclusion of this part, one can assume that if the distortion of all the NiO_6 octahedra in $\text{Li}_{0.98}\text{Ni}_{1.02}\text{O}_2$ is not able to distort cooperatively the rhombohedral lattice, the distortion of only a few of them in $\text{Li}_{0.63}\text{Ni}_{1.02}\text{O}_2$ cannot induce the observed macroscopic distortion. Therefore, the driving force of this structural distortion results from another phenomena. Since a lithium/vacancy ordering within the interslab space is likely to induce a symmetry decrease, an electron diffraction study has been carried out.

2.5. Electron diffraction study of the lithium/vacancy ordering

The electron diffraction experiments have been realized on both $\text{Li}_{0.98}\text{Ni}_{1.02}\text{O}_2$ and $\text{Li}_{0.63}\text{Ni}_{1.02}\text{O}_2$ phases [25]. In the case of the pristine material, the electron diffraction study confirms the XRD analysis, and all electron diffraction spots can be indexed with the classical hexagonal cell (space group: $R\bar{3}m$). On the contrary, for the de-intercalated phase many spots (with small intensity) cannot be indexed by considering the monoclinic cell deduced from the XRD (space group: $C2/m$). Fig. 4 gives an example of the reciprocal plane (zone axis [211]) obtained for the pristine $\text{Li}_{0.98}\text{Ni}_{1.02}\text{O}_2$ phase and the corresponding reciprocal plane (zone axis [001]) obtained for the $\text{Li}_{0.63}\text{Ni}_{1.02}\text{O}_2$ phase. The presence of these extra spots clearly indicates the existence of a larger unit cell which has been deduced from a complete analysis of the electron diffraction data. In order to propose a hypothesis on

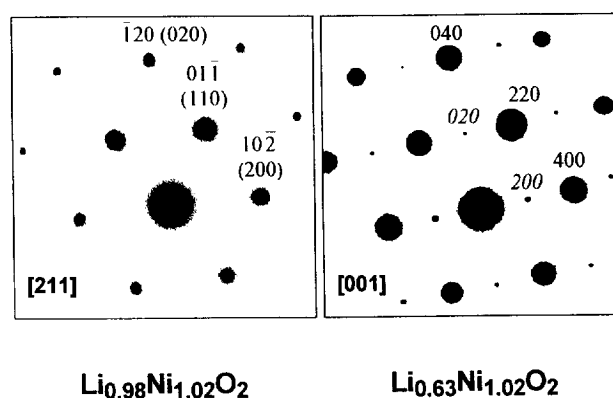


Fig. 4. Electron diffraction patterns of the $\text{Li}_{0.98}\text{Ni}_{1.02}\text{O}_2$ starting phase ([211] zone axis) and of the de-intercalated $\text{Li}_{0.63}\text{Ni}_{1.02}\text{O}_2$ phase ([001] zone axis). In the case of $\text{Li}_{0.98}\text{Ni}_{1.02}\text{O}_2$ both indexations are reported: $R\bar{3}m$ ($C2/m$). In the case of $\text{Li}_{0.63}\text{Ni}_{1.02}\text{O}_2$ a $2a_{\text{mon}} \times 2b_{\text{mon}} \times 2c_{\text{mon}}$ cell has been considered to index the superstructure spots.

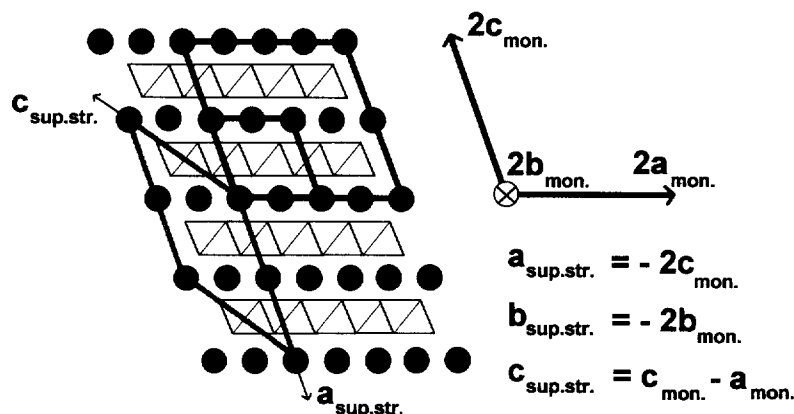
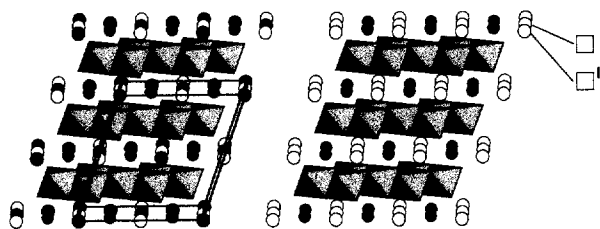


Fig. 5. Structural relationship between the monoclinic cell ($a_{\text{mon.}}$, $b_{\text{mon.}}$, $c_{\text{mon.}}$) deduced from the X-ray pattern, and the true superstructure cell ($a_{\text{sup.str.}}$, $b_{\text{sup.str.}}$, $c_{\text{sup.str.}}$), deduced from electron diffraction data. The larger superstructure cell ($2a_{\text{mon.}}$, $2b_{\text{mon.}}$, $2c_{\text{mon.}}$) used in the structure description is also represented.

the origin of the superstructure, a cell ($2a_{\text{mon.}} \times 2b_{\text{mon.}} \times 2c_{\text{mon.}}$) which is not the smallest one has been used. Nevertheless, it is convenient to use it, as it exhibits the same axis orientation as the one deduced from XRD without considering the superstructure. The geometric relations between these various cells are reported in Fig. 5. Considering this new cell, and in accordance with the XRD data, the superstructure of the $\text{Li}_{0.63}\text{Ni}_{1.02}\text{O}_2$ phase can be described with the non conventional $F2/m$ space group. The monoclinic cell parameters are: $a_{\text{mon.}} = 9.98 \text{ \AA}$, $b_{\text{mon.}} = 5.66 \text{ \AA}$, $c_{\text{mon.}} = 10.14 \text{ \AA}$, $\beta = 109.7^\circ$. The description of the layered structure of LiNiO_2 in this space group leads to consider three different lithium sites ($\text{Li}_{0.50}\text{Li}_{0.25}\text{Li}_{0.25}\text{NiO}_2$). If one assumes that they are not simultaneously and statistically occupied, an ordered superstructure within a large composition range may exist. For the composition limits of the monoclinic solid solution, the formulae can be written $\text{Li}_{0.50}\square_{0.25}\square'_{0.25}\text{NiO}_2$ and $\text{Li}_{0.50}\text{Li}_{0.25}\square'_{0.25}\text{NiO}_2$, respectively. A representation of these cationic distributions is given in Fig. 6. Moreover, it is important to note that this lithium/vacancy ordering within the interslab space is very sensitive to the presence of extra-nickel ions that tend to prevent the ordering. If their amount (z) is larger than or equal to 0.05, the monoclinic phase does not appear upon de-intercalation.

Another interesting result has been found during the electron diffraction study. It concerns the formation of twin crystals resulting from the rhombohedral/monoclinic tran-



$\text{Li}_{0.50}\text{Li}_{0.25}\square'_{0.25}\text{NiO}_2$ $\text{Li}_{0.50}\square_{0.25}\square'_{0.25}\text{NiO}_2$

Fig. 6. Lithium ordering in both end members of the monoclinic Li_xNiO_2 solid solution. The superstructure cell ($2a_{\text{mon.}}$, $2b_{\text{mon.}}$, $2c_{\text{mon.}}$) is also reported.

sition. At the structural transition, the monoclinic cell is formed in three equivalent directions related to the triangular lattice which characterizes the pristine phase. Upon de-intercalation, the topotactic nucleation of the monoclinic phase within the rhombohedral one must occur simultaneously and independently in several parts of the crystal. Therefore, all orientations of the monoclinic crystallites can be obtained in the same single crystal. The occurrence of this phenomenon is clearly identified on the electron diffraction patterns, since it induces, on some patterns, the apparition of characteristic double spot. This twin crystals formation constitutes an interesting point which must be studied in more detail in relation with the electrochemical behavior.

3. Conclusions

A general study of the short and long range structure of the pristine lithium nickel oxide and of the monoclinic partially de-intercalated phase has shown the complexity of the phenomena involved during the lithium de-intercalation/intercalation process. All these structural modifications which occur at various scales within the material are directly related to the overall electrochemical behavior and may play a peculiar role in the ageing processes.

Acknowledgements

The authors wish to thank P. Gravereau and M. Ménétrier for fruitful discussions and SAFT, AAR, CNES and Région Aquitaine for financial support.

References

- [1] M.G.S.R. Thomas, W.I.F. David, J.B. Goodenough and P. Groves, *Mater. Res. Bull.*, 20 (1985) 1137.
- [2] J.R. Dahn, U. Von Sacken, M.W. Juskow and J. Al-Janabi, *J. Electrochem. Soc.*, 138 (1991) 2207.

- [3] T. Ohzuku, H. Komori, M. Nagayama, K. Sawai and T. Hirai, *Chem. Express*, 6 (1991) 161.
- [4] T. Ohzuku, A. Ueda and M. Nagayama, *Solid State Ionics*, 69 (1994) 201.
- [5] W. Ebner, D. Fouchard and L. Xie, *Solid State Ionics*, 69 (1994) 238.
- [6] T. Ohzuku, in G. Pistoia (ed.), *Lithium Batteries*, Elsevier, Amsterdam, 1994, 239.
- [7] M. Broussely, F. Pertion, P. Biensan, J.M. Bodet, J. Labat, A. Lecerf, C. Delmas, A. Rougier and J.P. Pérès, *J. Power Sources*, 54 (1995) 109.
- [8] A. Lecerf, M. Broussely and J.P. Gabano, *Eur. Patent No. 0 345 707*; *US Patent No. 4 980 080* (1989).
- [9] A. Rougier, P. Gravereau and C. Delmas, *J. Electrochem. Soc.*, 143 (1996) 1168.
- [10] T. Ohzuku, A. Ueda and M. Nagayama, *J. Electrochem. Soc.*, 140 (1993) 1862.
- [11] W. Li, J.N. Reimers and J.R. Dahn, *Solid State Ionics*, 67 (1993) 123.
- [12] C. Delmas and I. Saadoune, *Solid State Ionics*, 53/56 (1992) 370.
- [13] C. Delmas, I. Saadoune and A. Rougier, *J. Power Sources*, 43/44 (1993) 595.
- [14] A. Ueda and T. Ohzuku, *J. Electrochem. Soc.*, 141 (1994) 2013.
- [15] T. Ohzuku, A. Ueda and M. Kouguchi, *J. Electrochem. Soc.*, 142 (1995) 4033.
- [16] J.N. Reimers, E. Rossen C.D. Jones and J.R. Dahn, *Solid State Ionics*, 61 (1993) 335.
- [17] E. Rossen, C.D. Jones and J.R. Dahn, *Solid State Ionics*, 57 (1992) 311.
- [18] A. Rougier, I. Saadoune, P. Gravereau, P. Willman and C. Delmas, *Solid State Ionics*, 90 (1996) 83.
- [19] J.P. Pérès, E. Suard and C. Delmas, submitted for publication.
- [20] J.P. Pérès, C. Delmas, A. Rougier, M. Broussely, F. Pertion, P. Biensan and P. Willman, *J. Phys. Chem. Solids*, 56 (1996).
- [21] J.P. Pérès, A. Demourgues and C. Delmas, *Solid State Ionics*, submitted for publication.
- [22] F. Capitaine and C. Delmas, *J. Electrochem. Soc.*, submitted for publication.
- [23] L.D. Dyer, B.S. Borie, J.R. and G.P. Smith, *J. Am. Chem. Soc.*, 76 (1954) 1499.
- [24] A. Rougier and C. Delmas, *Solid State Commun.*, 94 (1995) 123.
- [25] J.P. Pérès, F. Weill and C. Delmas, *Solid State Ionics*, submitted for publication.